Available online at www.sciencedirect.com
SCIENCE DIRECT
Polymer 46 (2005) 8838–8845
polymer
www.elsevier.com/locate/polymer

Micromechanical interpretation of the modulus of ethylene–(meth)acrylic acid copolymers

Katsuyuki Wakabayashi, Richard A. Register*

Department of Chemical Engineering, Princeton University, Princeton, NJ 08544-5263, USA

Received 14 October 2004; received in revised form 13 December 2004; accepted 15 December 2004
Available online 23 June 2005

Abstract

Statistical incorporation of a comonomer into polyethylene is well known to reduce its crystallinity, and consequently the small-strain modulus. However, we have found that when the comonomer is methacrylic or acrylic acid, the modulus of homogeneous copolymers initially decreases and then increases with increasing comonomer content. The modulus increase is traced to an elevation of the amorphous phase glass transition temperature (T_g) with comonomer content; T_g passes through room temperature at comonomer contents sufficiently low that substantial crystallinity remains. When the modulus is measured at temperatures above T_g, such that the amorphous phase is fully relaxed, a monotonic increase in modulus with crystallinity is both anticipated and observed. Several two-phase composite models are investigated to describe the modulus vs. crystallinity data above T_g; the Davies model provides a good quantitative description for the copolymers examined. The Davies model may also be applied at temperatures where the amorphous phase is incompletely relaxed, to extract its contribution to the semicrystalline polymer's modulus.

Keywords: Ethylene copolymer; Glass transition; Modulus

1. Introduction

Statistical incorporation of a comonomer into a crystallizable homopolymer dramatically influences the material's crystallinity, thermal behavior, and physical properties. Homogeneous copolymers of ethylene (E)—where the compositional variation between chains is minimal—can be synthesized either through coordination polymerization with single-site catalysts, as is frequently employed with hydrocarbon comonomers such as α-olefins (αO) and styrene (S) [1,2], or through classical high-pressure free radical polymerization, commonly employed to incorporate polar comonomers such as methacrylic acid (MAA) [1]. With such polymerization chemistries, a homogeneous product can be obtained in either a continuous stirred-tank reactor (provided the mixture is homogeneous), or a tubular reactor or fluidized bed (provided the conversion per pass is small). The structure–property relationships in these copolymers are of particular interest due both to their commercial importance and to the very substantial changes in physical properties, that can be achieved through variation in comonomer content.

The nature and extent of crystallinity, or the lack thereof, in such polymers are clearly important in defining their behavior. The effect of comonomer incorporation upon the melting point was originally treated by Flory [3], and subsequently crystallization thermodynamics and kinetics have been studied in depth [4–7]. The influence of the degree of crystallinity on mechanical properties has also been extensively studied [8–15]. Young's modulus, the tensile modulus in the small-strain limit, is perhaps the most basic such property, and thus represents an appropriate starting point for our investigation of the properties of ethylene–methacrylic acid and ethylene–acrylic acid (E/(M)AA) copolymers.

In homogeneous E/αO copolymers, the tensile modulus increases monotonically with crystalline volume fraction (or equivalently, with ethylene content, density, or crystalline weight fraction) [9–12]. A similar trend is found in ethylene–styrene (E/S) copolymers: the elastic modulus

* Corresponding author. Tel.: +1 609 258 4691; fax: +1 609 259 0211.
E-mail address: register@princeton.edu (R.A. Register).

0032-3861/$ - see front matter © 2005 Elsevier Ltd. All rights reserved.
doi:10.1016/j.polymer.2004.12.063

increases monotonically with crystallinity [13,14]. Such a dependence is easily understood in the framework of a two-phase composite model, since the crystallites should have a modulus some 10^3 times that of a rubbery amorphous phase: as comonomer content increases and crystallinity decreases, high-modulus crystalline regions are exchanged for low-modulus amorphous regions, and the overall modulus of the semicrystalline material is reduced.

Surprisingly, there have been very few studies on the structure–property relationships in homogeneous E/(M)AA copolymers, despite their widespread utilization both directly as copolymers, and as the partially neutralized salts, termed 'ionomers' [16]. Indeed, as we show below, E/(M)AA copolymers differ qualitatively from their well-studied E/αO and E/S counterparts in that their Young's modulus does not show a monotonic trend with crystallinity, but rather passes through a minimum. Our goals in the present work are first to explain this puzzling observation, and then to develop a quantitative model relating an E/(M)AA copolymer's microstructure (especially its crystallinity) to its modulus.

2. Experimental

2.1. Materials

A series of E/(M)AA copolymers and terpolymers were provided by DuPont; the terpolymers all incorporate *n*-butyl acrylate (*n*BA) to intentionally reduce polymer crystallinity. The sample code (e.g. E/9MAA/23.5*n*BA) indicates the nature and content of the acid comonomer (9MAA = 9 wt% MAA) and the content of the termonomer, if any (23.5*n*BA = 23.5 wt% *n*BA). The acid content was determined by titration, whereas the *n*BA content was found by FTIR, all at DuPont. These materials are produced by a high-pressure free radical polymerization process which yields little chemical heterogeneity between chains [17,18], though the polymers are highly polydisperse and contain both long-chain and short-chain branches. Copolymer pellets were melt-pressed into 0.2–0.5 mm thick sheets at 140 °C using a PHI hot press, followed by a quench to room temperature; the molded sheets were stored in a desiccator at room temperature for 2 days. ASTM D1708 dogbones were stamped from the sheets at room temperature for tensile testing; 7–10 mg specimens with the identical thermal history were prepared for differential scanning calorimetry (DSC). Copolymer samples were also pressed into 0.1 mm thick sheets for dynamic mechanical thermal analysis (DMTA), for which the sample dimensions are 6×23 mm^2.

2.2. Characterization

Uniaxial tensile stress–strain curves were obtained with an Instron Model 1122, equipped with an Environmental Chamber 3111 retrofitted to control the testing temperature within 0.3 °C, with a cycle time of 1 s. Measurements were taken at either 25 or 50 °C with the crosshead speed set at 2 in./min (engineering strain rate of 0.038 s^{-1}); strains were calculated from the crosshead displacement, corrected for the compliance of the load cell and grips. DSC was conducted with a Perkin–Elmer DSC-7 (with Pyris 1 software) equipped with an intracooler and calibrated with indium and tin; a heating ramp of 10 °C/min was used. DMTA was performed at 1 Hz on a Rheometrics RSA-II employing liquid nitrogen cooling, in tension mode (film fixture), using 5 °C temperature steps. The strain amplitude at low temperatures was 0.2%, increasing as the sample softened to maintain a minimum force of 10 g.

3. Results and discussion

3.1. Modulus at room temperature

The peak melting temperatures T_m determined by DSC are listed for all co- and terpolymers in Table 1. As expected for statistical heteropolymers, for a given co/termonomer, T_m decreases progressively with increasing co/termonomer content. Young's modulus (E) was obtained by calculating the slope of the elastic response in the small-strain regime ($\varepsilon < 5\%$) in a tensile stress–strain plot. The heat of melting, ΔH_{melt}, was obtained from the DSC traces, and converted to a weight fraction crystallinity by dividing by the heat of melting of fully crystalline polyethylene (278 J/g) [19]. The volume fraction of crystallites (ϕ_1) can be estimated from the weight fraction crystallinity following Marx and Cooper [20], using representative density values for the crystalline and amorphous regions of 1.00 and 0.91 g/cm^3. Though the actual amorphous phase density should vary by a few percent with polymer composition, the magnitude of this variation is no larger than the uncertainty in the measurement of ΔH_{melt}, since the endotherms in these statistical copolymers are broad. The values of E(25 °C) and ϕ_1 so determined are given in Table 1 for all polymers studied.

We will initially focus our discussion on the E/MAA copolymers, which form the most extensive series. Fig. 1 shows E(25 °C) vs. ϕ_1 for the E/MAA copolymers, plotted as solid symbols. Unlike E/αO and E/S copolymers, E(25 °C) first decreases, then increases, with polymer crystallinity. It is important to note that E(25 °C) is plotted on a logarithmic scale in Fig. 1; its variation across the range of crystallinities studied here is nearly an order of magnitude.

To interpret this result, we appeal to models for the modulus of isotropic two-phase composites. Such models attempt to describe the composite modulus as a function of the material properties of the two constituent phases, with the combining rule reflecting the topology or connectivity of the phases. In our case, the two phases should correspond to ethylene crystallites and amorphous regions; since the

Table 1
Characteristics of ethylene-based copolymers examined

Sample	Mole fraction ethylene	Peak T_m, °C	Young's modulus E(25 °C), MPa	Volume fraction crystallinity ϕ_1(25 °C)	T_g, °C
E/4MAA	0.987	109	220	0.41	1
E/6MAA	0.980	105	190	0.34	−1
E/9MAA	0.969	98	130	0.29	1
E/11.5 MAA	0.959	95	100	0.27	4
E/15 MAA	0.946	89	120	0.22	12
E/19 MAA	0.929	88	190	0.20	19
E/22 MAA	0.916	87	360	0.19	24
E/28 MAA	0.888	80	630	0.11	29
E/7 AA	0.972	108	210	0.37	14
E/12.5 AA	0.947	101	170	0.30	11
E/20 AA	0.911	77	60	0.14	24
E/8.5 AA/15.5 *n*BA	0.919	81	28	0.17	−20
E/9 MAA/23.5 *n*BA	0.886	72	15	0.14	−26

two are covalently bonded, good interdomain adhesion is assured. Thus, we anticipate that our materials should be describable through such a model (with the proper combining rule), provided that the properties of the crystallites and amorphous regions (which are assumed invariant with composition in such models) vary much less with composition than they differ from each other. As a starting point, we calculated rigorous upper and lower bounds on the copolymer moduli following the equations of Hashin and Shtrikman [21]:

$$E_{\text{comp}} = \frac{E_1E_2 + A(\phi_1E_1 + \phi_2E_2)}{A + \phi_2E_1 + \phi_1E_2} \tag{1}$$

$$A_{\text{upper}} = \frac{E_1(7 - 5\nu_1)}{8 - 10\nu_1} \tag{2}$$

$$A_{\text{lower}} = \frac{E_2(7 - 5\nu_2)}{8 - 10\nu_2} \tag{3}$$

where E_i is the elastic modulus, ϕ_i the volume fraction, and ν_i the Poisson's ratio of phase i ($E_1 > E_2$). The room-temperature values of E_i and ν_i for polyethylene reported by Janzen [15] (Fig. 1) were used to calculate the bounds shown as dashed curves in Fig. 1. Janzen's values were extracted from a statistical analysis of literature data for over 1100 polyethylenes; naturally, the result for E_1 (3800 MPa) rests principally on the highest-crystallinity samples, and that for E_2 (4 MPa) on the lowest-crystallinity samples, of which approximately 2/3 were high-pressure LDPE. It is apparent that one of the data points in Fig. 1 ($\phi_1 \approx 0.11$) lies above the Hashin–Shtrikman upper bound calculated with these parameters, suggesting that the true amorphous phase modulus may be significantly higher than the assumed value of 4 MPa.

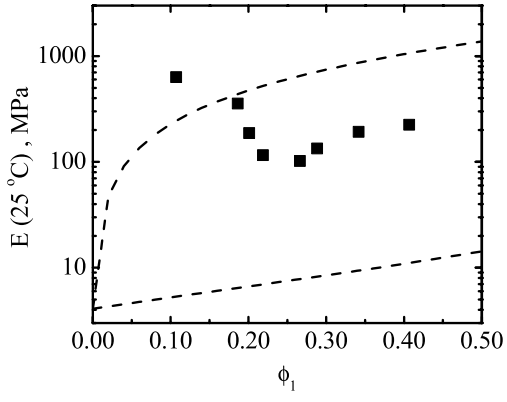

Fig. 1. Young's modulus of E/MAA copolymers 25 °C plotted against volume fraction crystallinity. Dashed curves are the upper and lower Hashin–Shtrikman bounds calculated with $E_1 = 3800$ MPa, $E_2 = 4$ MPa, $\nu_1 = 0.42$, and $\nu_2 = 0.50$.

While some variation in E/MAA amorphous phase modulus with composition may result from changes in hydrogen bonding or entanglement molecular weight as the MAA content changes, these minor influences seem implausible as the source of the large, nonmonotonic variation in modulus shown in Fig. 1. Rather, this variation seems more characteristic of vitrification/devitrification, which changes the modulus of the amorphous phase by a factor of order 10^3. The broad melting endotherms in our materials obscured any evidence of a glass transition in the DSC traces; DMTA was more useful in this regard. Fig. 2 plots the tensile storage modulus (E'), loss modulus (E''), and loss tangent ($\tan\delta$) for four representative E/MAA copolymers (9–28 wt% MAA). All show a single, reasonably narrow peak in E'' and $\tan\delta$, accompanied by a decrease in E' by 1–2 orders of magnitude. We took the E'' peak temperature as a measure of the glass transition temperature (T_g), and list these values in Table 1 for all materials examined.

The data in Table 1 reveal a general increase in T_g as the (M)AA content is increased. This trend is shown graphically in Fig. 3 for the E/MAA series, where T_g is plotted against the weight fraction of MAA in the amorphous phase, determined by mass balance from the measured ϕ_1, assuming complete exclusion of MAA from the crystals. The general trend in the data is reminiscent of the Fox

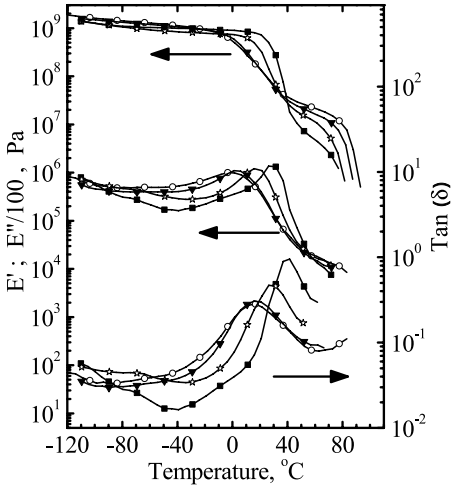

Fig. 2. Dynamic moduli and loss tangent vs. temperature for selected E/MAA copolymers, obtained from DMTA at 1 Hz. (○) 9%, (▼) 11, (☆) 15, (■) 28 wt% MAA; every third data point is decorated with a symbol for clarity.

equation [22]:

$$\frac{1}{T_{g,mixture}} = \frac{w_1}{T_{g1}} + \frac{w_2}{T_{g2}} \tag{4}$$

where w_i is the weight fraction of component i. For comparison, the dashed curve in Fig. 3 was calculated according to Eq. (4) with $T_{g2}=501$ K (228 °C, T_g for PMAA [23]) and $T_{g1}=251$ K (−22 °C, the E'' peak for the β transition measured on an LDPE homopolymer polymerized under similar conditions; these LDPE DMTA data are shown in Fig. 4). Surprisingly, the Fox equation with these parameter values reproduces our measured T_g values within 6 °C for the polymers having 9–28 wt% MAA (filled symbols in Fig. 3). However, we do not assign any fundamental significance to this observation, since (1) several ethylene copolymer systems studied in the literature do not show a Fox-like dependence on composition, but rather exhibit a minimum when T_β and T_g are plotted against composition [9,13,24], and (2) inspection of Table 1 shows that E/AA copolymers with 10–20 wt% AA have T_g values quite similar to those of the E/MAA copolymers of similar comonomer weight fraction, despite the fact that PAA has a much lower T_g (106 °C [25]) than PMAA. Deviations from Fox-like behavior can be seen in Fig. 3 at lower MAA contents (below 10 wt% MAA in amorphous phase, open symbols), where the T_g appears to pass through a minimum. As shown by the DMTA data in Fig. 4, these two polymers are sufficiently crystalline that they show signs of a developing α relaxation, as in the LDPE homopolymer (data shown in Fig. 4). By contrast, E/MAA copolymers with nine or more wt% MAA (Fig. 2) show a single relaxation peak, as is commonly found in ethylene copolymers with thin polyethylene crystals (<6 nm) [26]—though such polymers may nevertheless retain a significant degree of crystallinity, as is the case for our polymers.

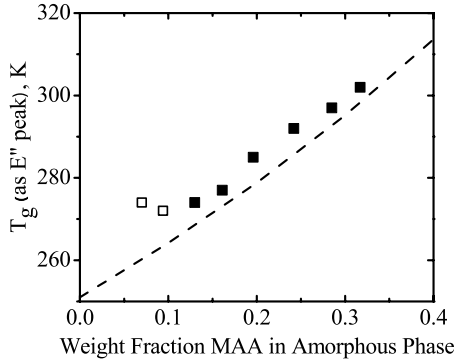

Fig. 3. Glass transition temperature of E/MAA copolymers (E'' maxima) plotted against weight fraction MAA in amorphous phase. Unfilled symbols represent copolymers with low MAA content (≤6 wt%), whose DMTA curves indicate the emergence of an α relaxation. Dashed curve is the Fox equation, with pure-component values assigned as $T_{g1}=251$ K and $T_{g2}=501$ K.

Fig. 3 shows that several of the E/MAA copolymers have glass transitions in the vicinity of room temperature; these copolymers should thus have an amorphous phase modulus (hence a composite modulus) significantly higher than if the amorphous phase were fully relaxed. This explains the unexpected increase in E(25 °C) at low ϕ_1 evident on the left side of Fig. 1, along with the point whose modulus exceeds the Hashin–Shtrikman upper bound calculated with $E_2=$ 4 MPa (the fully-relaxed value). By contrast, the increase in E(25 °C) at high ϕ_1 on the right side of Fig. 1 is due to the usual increase in modulus with crystallinity, as observed in E/αO and E/S copolymers [9–14]. These two factors combine to produce the initially puzzling minimum observed in E(25 °C) vs. ϕ_1.

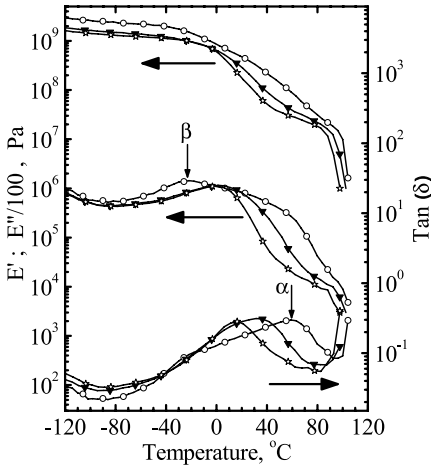

Fig. 4. Loss modulus and loss tangent vs. temperature for LDPE and E/MAA copolymers with low MAA content (≤6 wt%), obtained from DMTA at 1 Hz. (○) LDPE homopolymer, (▼) 4, (☆) 6 wt% MAA; every third data point is decorated with a symbol for clarity. The α and β transition maxima for the LDPE homopolymer are indicated with vertical arrows above the tan δ and E'' curves, respectively (where each transition is most evident).

Of course, for comonomers which form a homopolymer that is glassy at room temperature, an eventual increase in E(25 °C) with comonomer content is expected, once the copolymer's T_g rises through room temperature. The distinguishing feature of MAA and AA as comonomers is that they elevate T_g quite rapidly, so that T_g reaches room temperature at a comonomer content which still allows for substantial crystallinity. By comparison, to raise the T_g of an E/S copolymer above room temperature, so much S must be incorporated ($\approx$70 wt%) that all crystallinity is lost [13]. A similar situation pertains for homogeneous atactic ethylene–norbornene (E/N) copolymers, where E'(25 °C) initially drops as the N content is increased (up to 18 wt% N), and only begins to increase after all crystallinity is lost [27]. By contrast, 19 wt% MAA is sufficient to raise T_g to room temperature, while still preserving 20 vol% crystallinity in the copolymer. We are unaware of any other statistical ethylene copolymers showing this behavior.

3.2. Modulus at elevated temperature

Any model for the moduli of E/MAA copolymers must thus account for both of these effects, which are most easily separated by ensuring that the amorphous phase is fully relaxed during the modulus measurement. Therefore, we also measured the moduli of E/MAA copolymers at 50 °C, as all copolymers' E' curves approach a plateau at this temperature (Figs. 2 and 4); therefore, the amorphous phase in all the copolymers should be fully relaxed. As noted previously [20], these copolymers contain 'secondary' crystallites which melt at temperatures below 50 °C; an approximate correction for this effect was made by recalculating ϕ_1 at 50 °C by integrating the DSC enthalpy from 50 °C to the final melting temperature. Fig. 5 presents E(50 °C) vs. ϕ_1 for the same E/MAA copolymers, and indeed, the expected monotonic increase of E with ϕ_1 is observed.

At 50 °C, then, it should be reasonable to approximate the modulus of the amorphous phase as invariant with composition, and to evaluate the applicability of two-phase composite models to the data in Fig. 5. Kerner's [28] original treatment, Eq. (1), was based on a morphology of spherical fillers of one phase dispersed in a matrix of the other. The Hashin–Shtrikman bounds, Eqs. (2) and (3), employ the Kerner equation with values of A which correspond to the composite having either the high- or low-modulus component as the matrix. Generalized Kerner-type models permit other forms for A, frequently more complex, to reflect the connectivity of the phases. One variation is the self-consistent Budiansky model, which describes a system undergoing phase inversion (as ϕ_1 is increased from zero to unity) [29]:

$$A = \frac{E_{comp}(7 - 5\nu_C)}{8 - 10\nu_C} \tag{5}$$

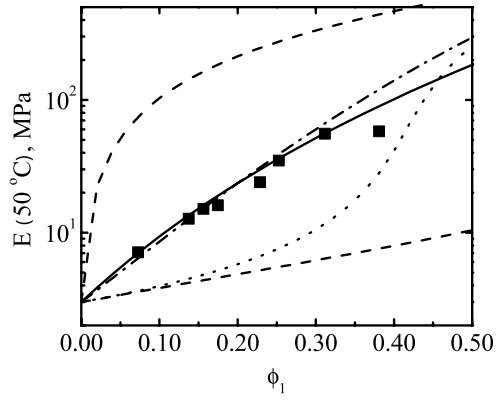

Fig. 5. Young's modulus of E/MAA copolymers at 50 °C plotted against volume fraction crystallinity. The continuous curves represent the predictions of several two-phase composite models, calculated with E_1 = 1700 MPa, E_2 = 3 MPa, ν_1 = 0.42, and ν_2 = 0.50. (– –) Hashin–Shtrikman bounds, (- - -) Budiansky model, (– -) Halpin–Tsai–Sehanobish model, (—) Davies model.

where ν_C is the weighted average of the Poisson's ratios of the two phases. The Halpin–Tsai model considers the crystallites as anisometric inclusions in a continuous matrix [30,31]:

$$A = \zeta E_2 \tag{6}$$

In Eq. (6), ζ is a parameter that reflects the aspect ratio of the inclusions. For systems such as fiber- or flake-reinforced composites, ζ might be a constant subject to independent measurement, but for semicrystalline copolymers, it is unclear what the appropriate value of ζ would be, or even if it is invariant with composition (crystallinity). Based on the moduli for a series of E/αO copolymers, Sehanobish et al. [10] proposed the correlation $\zeta = 4.7 \exp(5.5\phi_1)$, implying that the effective aspect ratio of the crystals increases with crystallinity.

A qualitatively different model is the Davies equation [32], which was developed by considering local variations in composition about the average volume fraction in a Kerner-type structure:

$$E_{comp}^{1/5} = \phi_1 E_1^{1/5} + \phi_2 E_2^{1/5} \tag{7}$$

Eq. (7) is a particular solution to the differential equation which results, applicable when the bulk moduli of the phases are identical; since the bulk moduli of crystalline and amorphous polyethylene differ by less than a factor of three [15], this is a reasonable approximation. The form of Eq. (7), where the composite modulus diverges when the modulus of either component diverges, implies cocontinuity of the phases.

In Fig. 5, the Hashin–Shtrikman bounds, and the predictions of the Budiansky, Halpin–Tsai and Davies models are shown as continuous curves. Not surprisingly, the data fall roughly midway between the Hashin–Shtrikman bounds, so neither bound provides a good correlation. The Budiansky model also describes the data poorly; though

this model was favored by Janzen [15] to describe the modulus of polyethylenes over a broad crystallinity range, it systematically and substantially underpredicts the modulus in the low-crystallinity range ($\phi_1 < 0.4$) relevant here. Moreover, as Fig. 5 shows, the Budiansky model predicts a much more rapid change between low- and high-modulus materials (characteristic of phase inversion, and the transition between Hashin–Shtrikman lower-bound and upper-bound behavior) than is seen experimentally.

By contrast, both the Halpin–Tsai equation (with the Sehanobish correlation) and the Davies equation adequately describe the modulus at low values of ϕ_1 (< 0.25). However, for $\phi_1 > 0.3$, the Davies model describes the experimental data more accurately, and the simplicity of the Davies equation is an additional asset. The success of the Davies equation is perhaps unsurprising, since the large aspect ratio and growth habit of lamellar crystallites produce nearly co-continuous amorphous and crystalline phases over a very broad range of ϕ_1. Janzen [15] made the 'curious observation' that the Davies equation described the 'lower family' of modulus data (for lower-crystallinity resins) well; nonetheless, he did not investigate this model further. Nielsen [33] reported that the Davies equation adequately correlated data for a variety of linear polyethylenes and ethylene copolymers over a broad range of crystallinity, though the deviations of some materials' moduli from the Davies model fit was quite large (a factor of four), and an unrealistically low value of the amorphous phase modulus ($E_2 = 0.7$ MPa) was required to obtain the best fit to the data. This may explain why the Davies equation has largely been overlooked as a useful descriptor of the modulus of semicrystalline polymers. We note that the close agreement between the Halpin–Tsai–Sehanobish equation and the Davies equation curves in Fig. 5 indicates that the moduli of the E/αO copolymers studied by Sehanobish et al. [10] would be equally well-described by the Davies equation. These results suggest that the Davies model may well be generally applicable to polymers of low to moderate crystallinity, though this will require further investigation.

The parameter values used for the calculations in Fig. 4 merit some discussion. The value of $E_1 = 1700$ MPa was obtained by scaling Janzen's value at 25 °C($E_1 = 3800$ MPa) by the measured ratio of the moduli for a specimen of high-density polyethylene at 25 and 50 °C. This is a rough approximation, but since all our materials are far away from $\phi_1 = 1$, the calculated values of E_{comp} are not strongly dependent on E_1 in any case. For E_2, 3 MPa was obtained as the best fit of the Davies and Halpin–Tsai–Sehanobish models to the data; the other three models differ too radically from the data to provide a sensible best fit. This value of E_2 is less than the value found by Janzen [15] for LDPE at room temperature (4 MPa, with the suggestion that the extrapolation was sufficiently uncertain that the actual value could be as much as an order of magnitude larger). Based on simple rubber elasticity theory, with the notion that the crystallites are junction points and all amorphous phase chains are elastically active strands, one would expect that E_2 should increase as temperature is increased, not decrease. But in fact, not all amorphous chains are elastically active; both LDPE and our E/MAA copolymers possess a hyperbranched molecular structure, with many branches that are only a few entanglement spacings long. If not tied into a crystallite, such branches will eventually disentangle and make no contribution to the modulus at long times; at a fixed strain rate (as in our experiments), the fraction of these chains that disentangle faster than the measurement rate will increase with increasing temperature, hence the measured modulus will decrease.

We recall that the assumption of a composition-independent E_2 even at 50 °C implies that the amorphous phase is fully relaxed at this temperature—or, at least, that any constraints that the crystals impose on amorphous phase relaxation are similar across the series of materials. This may not be true for polyethylenes in general; the mechanical strength of the α relaxation is quite large, as thoroughly demonstrated by Boyd [34], and the temperature of the α relaxation increases with crystal thickness [26]. For statistical copolymers, crystal thickness (hence T_α) and degree of crystallinity (ϕ_1) are inherently correlated; thus, as ϕ_1 is increased, T_α will eventually increase through the measurement temperature, yielding an E_2 (at fixed temperature) which increases with ϕ_1, as discussed previously by Crist et al. [7]. This may explain the apparent success of the Budiansky model in describing polyethylenes of higher crystallinity [15], where the higher moduli predicted by the Budiansky vs. Davies model at high ϕ_1 (beyond the range of calculation in Fig. 5) may in fact reflect a higher value of E_2 at high ϕ_1, rather than a change in phase continuity.

Having established the validity of the Davies model for E/MAA copolymers when $T_g < T < T_m$, we now examine the behavior of related homogeneous ethylene co- and terpolymers: E/AA, E/MAA/*n*BA and E/AA/*n*BA. Exchanging MAA for AA or *n*BA should not produce any qualitative change in the microstructure of the material, so we expect them to follow the same combining rule, i.e. the Davies equation. For $T_g < T < T_m$, the modulus of these materials should differ only modestly from that of an E/MAA copolymer with the same ϕ_1, due to differences in E_2 (such as through entanglement molecular weight of the amorphous heteropolymer chains). Fig. 6 shows E(50 °C) vs. ϕ_1 for these additional co- and terpolymers, with the Davies equation fit for the E/MAA series shown for reference as the solid curve. The points for the three E/AA copolymers lie systematically below the E/MAA curve, but are satisfactorily described by the Davies equation with $E_2 = 1.7$ MPa, shown as the dot-dashed curve. The reason for this modest but systematic difference is not entirely clear; the obvious implication is that exchanging MAA for AA units along the chain yields a lower plateau modulus. The thermal instability of PMAA and PAA homopolymers prevents a direct measure of their

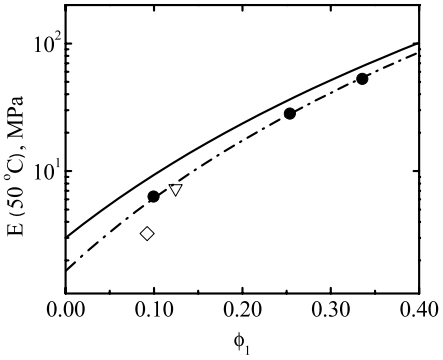

Fig. 6. Young's modulus of other ethylene-based co- and terpolymers at 50 °C plotted against volume fraction crystallinity. (●) E/AA copolymers, (▽) E/8.5AA/15.5*n*BA terpolymer, (◇) E/9MAA/23.5*n*BA terpolymer. (—) Davies equation fit to E/MAA copolymers, from Fig. 5 (E_1 = 1700 MPa, E_2 = 3 MPa). (– -) best Davies equation fit to E/AA copolymers (E_1 = 1700 MPa, E_2 = 1.7 MPa).

plateau moduli, though it is known that the methyl [35] and *n*-butyl [36] esters of PAA have lower plateau moduli than the analogous PMAA esters. An effect likely to be more important is that acrylate hydrogens (absent when the comonomer is MAA) are easily abstracted during high-pressure free-radical polymerization, leading to more extensive short- and long-chain branching, as confirmed through ^{1}H NMR analyses of E/MAA, E/AA, and E/*n*BA copolymers [37]. Short-chain branching will lead to a reduced entanglement density at any test rate, while a more hyperbranched structure will increase the fraction of the polymer chains which can disentangle during the modulus measurement.

Returning to Fig. 6, the terpolymers E/9MAA/23.5*n*BA and E/8.5AA/15.5*n*BA both have substantially lower values of E(50 °C) than the E/MAA copolymers, reflecting a much lower E_2(50 °C); moreover, with increasing *n*BA content, the values of E(50 °C) for the terpolymers lie further below the line which describes the E/MAA copolymers. Extra branching through the acrylate units should be important here as well, but in addition, the low plateau modulus of P*n*BA homopolymer (approximately E = 0.19 MPa [36]) certainly contributes to the lower value of E_2 for the terpolymers. Thus, the fact that the points in Fig. 6 for the E/AA copolymers and the *n*BA-containing terpolymers do not superimpose on the curve found for E/MAA copolymers does not indicate a lack of general applicability of the Davies equation to such polymers; it simply indicates that these other polymers have different (lower) values of E_2.

Finally, we note that the Davies model should apply to our materials at any temperature, not just 50 °C, because the connectivity of the phases implicit in Eq. (7) should not change with temperature. Modest changes with crystallinity with temperature are accounted for through ϕ_1, just as co- or termonomer content changes ϕ_1, while still obeying Eq. (7). Thus, we can use Eq. (7) to extract the amorphous-phase modulus E_2 from the measured value of E_{comp} at any temperature, since E_1 is known or estimable. The room-temperature (25 °C) data in Fig. 1 are obviously of particular interest; Fig. 7 shows the values of E_2(25 °C) calculated from E_{comp}(25 °C), using Janzen's value of E_1(25 °C) = 3800 MPa. Values of E_2(25 °C) are plotted against comonomer content in panel (a), and against amorphous-phase T_g in panel (b). Both panels show that at low MAA content (low T_g), E_2 is essentially constant, with an average value of 10 MPa. This value is significantly higher than the value of E_2 = 3 MPa determined at 50 °C, as discussed above; it is compatible with Janzen's value (4 MPa) within its stated uncertainty, and is only slightly higher than the values of melt modulus (7–8 MPa) reported by Krigas et al. [9] for linear polyethylene and copolymers with short-branch content similar to LDPE. At higher comonomer contents, the influence of the amorphous-phase T_g becomes apparent, with the amorphous-phase modulus increasing by nearly two orders of magnitude for the highest-MAA content polymer. Note that the actual values of E_2(25 °C) for these highest-MAA content polymers may be even higher than shown in Fig. 7, since when T_g exceeds room temperature, the amorphous phase can undergo physical aging. This aging process leads to an enthalpy relaxation near T_g in the DSC traces which our procedure interprets as a contribution to the enthalpy of melting, thus generating artificially high values of ϕ_1 (and low values of E_2, via Eq. (7)) if substantial physical aging occurs. We are currently

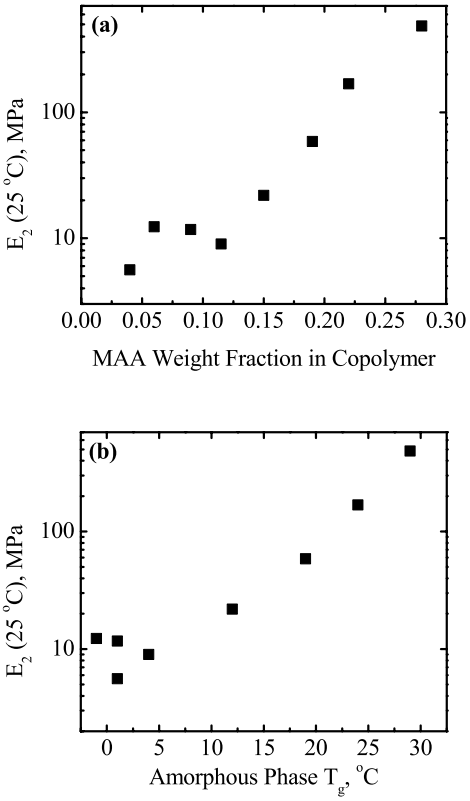

Fig. 7. Amorphous phase modulus, E_2, of E/MAA copolymers at 25 °C plotted against (a) comonomer (MAA) content; (b) amorphous phase T_g (DMTA E'' peak temperature). E_2 values remain low and essentially constant until the copolymer's T_g approaches room temperature.

investigating this possibility for high-acid E/MAA copolymers.

4. Conclusions

We have found that the modulus of a wide variety of low- to medium-crystallinity ethylene copolymers can be effectively described by perhaps the simplest combining rule for two-phase composites: the Davies equation. For such a two-phase composite model to be useful, the properties of the two phases (crystallites and amorphous interlayers) should be nearly invariant with composition, a condition which is satisfactorily obeyed at room temperature by copolymers of ethylene with α-olefins and even styrene, studied in previous literature reports. However, when the comonomer is acrylic or methacrylic acid, the amorphous-phase T_g increases rapidly with comonomer content and rises through room temperature even though substantial crystallinity remains; vitrification of the amorphous phase, in turn, produces a marked increase in the modulus of the semicrystalline copolymer, and a nonmonotonic dependence of modulus on comonomer content. For the series of E/MAA copolymers studied, crystallinity and vitrification of the amorphous phase make comparable contributions to the modulus, mandating a quantitative separation of these two effects. By inverting the Davies equation, the amorphous phase modulus E_2 may be determined at any temperature, whether relaxed or not. The ability to determine the amorphous phase modulus in a semicrystalline copolymer is an important step in the development of fundamental structure–property relationships in these materials.

Acknowledgements

This work was generously supported by DuPont Packaging and Industrial Polymers, Sabine River Works. Materials were provided by Brian Roach and Drs John Paul, John Chen, and George Prejean of DuPont, and by Yoshimasa Yamamoto of Mitsui-DuPont Polymers (E/AA20). The authors are especially grateful to Dr Paul for guidance at the outset of this work, and for stimulating discussions throughout.

References

[1] Peacock AJ. Handbook of polyethylene: structures, properties, and applications. New York: Marcel Dekker; 2000.
[2] Kaminsky W. Adv Catal 2002;46:89–159.
[3] Flory PJ. Trans Faraday Soc 1955;51:848–57.
[4] Alamo RG, Mandelkern L. Macromolecules 1991;24:6480–93.
[5] Alizadeh A, Richardson L, Xu J, McCartney S, Marand H, Cheung YW, et al. Macromolecules 1999;32:6221–35.
[6] Crist B, Howard PR. Macromolecules 1999;32:3057–67.
[7] Crist B. Polymer 2003;44:4563–72.
[8] Crist B, Fisher CJ, Howard PR. Macromolecules 1989;22:1709–18.
[9] Krigas TM, Carella JM, Struglinski MJ, Crist B, Graessley WW, Schilling FC. J Polym Sci, Polym Phys Ed 1985;23:509–20.
[10] Sehanobish K, Patel RM, Croft BA, Chum SP, Kao CI. J Appl Polym Sci 1994;51:887–94.
[11] Kennedy MA, Peacock AJ, Failla MD, Lucas JC, Mandelkern L. Macromolecules 1995;28:1407–21.
[12] Hu WG, Srinivas S, Sirota EB. Macromolecules 2002;35:5013–24.
[13] Chen H, Guest MJ, Chum S, Hiltner A, Baer E. J Appl Polym Sci 1998;70:109–19.
[14] Lobbrecht A, Friedrich C, Sernetz FG, Mulhaupt R. J Appl Polym Sci 1997;65:209–15.
[15] Janzen J. Polym Eng Sci 1992;32:1242–54.
[16] Longworth R, Nagel H. In: Tant MR, Mauritz KA, Wilkes GL, editors. Ionomers: synthesis, structure, properties and applications. New York: Blackie Academic and Professional; 1997. p. 365–89.
[17] Vanhoorne P, Register RA. Macromolecules 1996;29:598–604.
[18] Longworth R. In: Holliday L, editor. Ionic polymers. New York: Wiley; 1975. p. 69–172.
[19] Wunderlich B. Macromolecular Physics. New York: Academic Press; 1973.
[20] Marx CL, Cooper SL. J Macromol Sci Phys 1974;B9:19–33.
[21] Hashin Z, Shtrikman S. J Mech Phys Solids 1963;11:127–40.
[22] Fox TG. Bull Am Phys Soc 1956;1:123.
[23] Razinskaya IN, Kharitonova NE, Shtarkman BP. Vysokomol Soedin B 1969;11:892–4.
[24] Popli R, Mandelkern L. Polym Bull 1983;9:260–7.
[25] Hughes LJT, Fordyce DB. J Polym Sci 1956;22:509–26.
[26] Popli R, Glotin M, Mandelkern L, Benson RS. J Polym Sci, Polym Phys Ed 1984;22:407–48.
[27] Wilson TP, Von Dohlen WC, Koleske JV. J Polym Sci, Polym Phys Ed 1974;12:1607–18.
[28] Kerner EH. Proc Phys Soc London B 1956;69:808–13.
[29] Budiansky B. J Mech Phys Solids 1965;13:223–7.
[30] Halpin JC, Kardos JL. J Appl Phys 1972;43:2235–41.
[31] Tsai SW. Plast Polym 1969;37:391–5.
[32] Davies WEA. J Phys D Appl Phys 1971;4:1176–81.
[33] Nielsen LE. J Appl Polym Sci 1975;19:1485–6.
[34] Boyd RH. Macromolecules 1984;17:903–11.
[35] Fetters LJ, Lohse DJ, Graessley WW. J Polym Sci B, Polym Phys 1999;37:1023–33.
[36] Hrouz J, Janacek J. J Polym Sci A-2 1972;10:1383–95.
[37] McCord EF, Shaw WH, Hutchinson RA. Macromolecules 1997;30: 246–56.